Scientific paper

# Synthesis, Characterization and DFT Study of Ti(IV) Phthalocyanines with Quinoline Groups

Seyda Aydogdu, Oznur Dulger Kutlu, Ali Erdogmus and Arzu Hatipoglu\* o

Department of Chemistry, Yildiz Technical University, 34220, Istanbul, Turkey

\* Corresponding author: E-mail: hatiparzu@yahoo.com

Received: 05-18-2024

#### **Abstract**

The synthesis, characterization, and electronic properties of 4-((7-methoxyquinolin-4-yl)oxy), 4-(quinolin-2-ylthio), and 4-((7-(trifluoromethyl)quinolin-4-yl)thio) peripherally substituted oxo-titanium phthalocyanines are described for the first time. The structures of the compounds were determined by UV-Vis, FTIR, <sup>1</sup>H NMR, and MALDI-TOF mass spectrometry. Electronic spectra and molecular and electronic properties of compounds were calculated by Density Functional Theory (DFT) and Time-Dependent Density Functional Theory (TD-DFT) methods. Solvent effects on the electronic, geometric, and reactivity properties of the compounds were also investigated. Global and local reactivity indices and Molecular Electrostatic Potential surfaces of compounds were calculated. The reactivities and electronic structures of molecules vary depending on the solvent and substituents. It has been found that the synthesized compounds can be used for different purposes such as dye-sensitized solar cells and photodynamic therapy applications.

Keywords: Oxo-titanium phthalocyanine, synthesis, Density Functional Theory, solvent effect.

#### 1. Introduction

Phthalocyanines (Pcs) are  $18 \pi$  electron ring systems that are composed of four isoindole units bridged with aza nitrogen atoms. 1 It has 18 delocalized electrons that are responsible for its strong absorption in the visible spectrum domain and also they have the high thermal and chemical stability.<sup>2</sup> Thus, Pcs with their tunable chemical properties can be good candidates for use in photodynamic therapy, gas sensors, organic field transistors, or dye sensitized solar cells.<sup>3,4</sup> These in turn, lead to high interest to Pc compounds and studies about variation in the chemical structure of Pcs have been reported in the last years. In the literature, there are lots of Pc papers about different synthesizing method and their applications.<sup>5-13</sup> With the increasing popularity of theoretical methods there are also some studies that performed by using DFT to understand electronic properties of Pcs. 14-17 Although, knowledge and understanding of different substituent and solvents effects on the Pcs properties are still not sufficient.

There is a need for experimental and theoretical studies on new types of Pcs for finding desired properties. One of the most desired properties of a compound is to have a red-shifted absorption spectrum. Because these types of compounds can be used in photodynamic therapy and dye sensitzed solar cell areas. 18,19 The shift is more

prominent with electron-donating substituents such as – OR and –SR, etc. A closely related practical method of obtaining a red-shift is by introduction of special metal ions such as TiO<sup>2+</sup>.<sup>20</sup> Quinoline is a heterocyclic compound containing aromatic nitrogen and water-soluble compounds are obtained by methylation of nitrogen atoms in its structure using appropriate agents.<sup>20</sup> It is also known that trifluoromethyl group is prominent for medicinal chemistry applications.<sup>21</sup> Owing to the importance of different groups on the reactivity of compounds, a comprehensive research for quinolin and trifluoromethyl group containing compounds is desired.

The properties of compounds depend on their electronic structures. Various properties of compounds can be calculated with quantum chemical methods. Quantum chemical methods allow experimental results to be explained and information can be obtained in cases where some experimental data are not available. The usage of experimental and theoretical methods together lead to obtain more robust scientific datas and new discoveries. 22,23 In recent years, Density Functional Theory (DFT) has been widely used to effectively find the optimum electronic structure, structural parameters and various properties. 24,25 It is very important to know the structural and electronic properties of newly synthesized compounds so that they can be used in different areas.

The main purpose of this study is to determine the electronic, geometric and reactivity properties of Pcs containing different quinoline-derived substituents. For this purpose, 4-((7-methoxyquinolin-4-yl)oxy), 4-(quinolin-2-ylthio) and 4-((7-(trifluoromehyl)quinolin-4-yl) thio) phthalonitriles and their oxo-titanium phthalocyanine derivatives were synthesized and characterized. The effects of substituent and solvents on the spectral performance properties of newly synthesized complexes were investigated. DFT and TD-DFT studies were used to understand the electronic transitions nature of compounds. We also conducted local reactivity descriptor analysis for deeper understanding prominent reactive sites of the compounds. At the same time, the calculation results were used to interpret their possible usage areas.

#### 2. Experimental

### 2. 1. Materials and Equipment in the Experiments

All reagents and solvents were of reagent grade quality and were obtained from commercial suppliers. Absorption spectra in the UV-visible region were recorded with a Shimadzu 2001 UV spectrophotometer. FT-IR spectra were measured with a Perkin Elmer Spectrum One Spectrometer. The mass spectra were acquired on a Bruker Daltonics (Bremen, Germany) Microflex mass spectrometer equipped with an electron spray ionization (ESI) source. <sup>1</sup>H-NMR spectra were recorded on a Varian 500 MHz spectrometer.

#### 2. 2. Synthesis

### 2. 2. 1. General Procedure for the Aynthesis of Phthalonitrile Derivatives (1-3)

Substituted quinoline derivatives 7-methoxyquino-lin-4-ol (0.9 mmol), quinoline-2-thiol (1.24 mmol) and 7-(trifluoromethyl)quinoline-4-thiol (0.8 mmol) were dissolved in dry DMF. To this reaction mixture 4-nitrophthalonitrile (1.25 mmol) and anhydrous K<sub>2</sub>CO<sub>3</sub> (6.0 mmol) were added under Ar atmosphere. The resulting reaction mixture was stirred at room temperature for 24 h. The reaction was monitored by TLC and then allowed to cool to room temperature. The reaction mixture was poured into cold water (100 mL) and filtered. The precipitate washed with H<sub>2</sub>O and diethyl ether, then dried. The residue was recrystallized from ethanol to obtain pure phthalonitrile derivatives.

#### 4-(7-methoxyquinolin-4-yl)oxy)phthalonitrile (1)

Yield: 0.31 g (85%). FT-IR (ATR) (cm<sup>-1</sup>): 3073–3031 (Ar. C–H), 2965- 2831 (Aliph. C–H), 2239 (C≡N), 1272 (C–O–C). <sup>1</sup>H NMR (500 MHz, DMSO $d_6$ ) (δ: ppm): 8.76 (s, 1H, Ar-H), 8.22-8.06 (m, 3H, Ar-H), 7.74 (s, 1H, Ar-H),

7.48 (s, 1H, Ar-H), 7.33 (s, 1H, Ar-H), 6.91 (s, 1H, Ar-H), 3.95 (s, 3H). MALDI-TOF-MS (m/z): calcd. 301.298 for  $C_{18}H_{11}N_3O_2$ ; found 301.687 [M]<sup>+</sup>.

#### 4-(quinolin-2-ylthio)phthalonitrile (2)

Yield: 0.35 g (85%). FT-IR (ATR) (cm-1): 3114-3073 (Ar. C-H), 2229 (C $\equiv$ N), 1498, 1421, 1292, 1137 (C-S-C). 1H NMR (500 MHz, Chloroformd) ( $\delta$ : ppm): 8.18-8.16 (m, 2H, Ar-H), 8.01-7-97 (m, 2H, Ar-H), 7.89-7.84 (m, 2H, Ar-H), 7.81-7.78 (m, 1H, Ar-H), 7.65-7.61 (m, 1H, Ar-H), 7.42-7.41 (d, 1H, Ar-H). MALDI-TOF-MS (m/z): calcd. 287.338 for C17H9N3S; found 286.00 [M]+.

### 4-((7-(trifluoromethyl)quinolin-4-yl)thio) phthalonitrile (3)

Yield: 0.26 g (88%). FT-IR (ATR) (cm $^{-1}$ ): 3099-3027 (Ar. C–H), 2235 (C≡N), 1500, 1477, 1284, 1150 (C–S–C). <sup>1</sup>H NMR (500 MHz, Chloroform*d*) ( $\delta$ : ppm): 9.02 (s, 1H, Ar-H), 8.55 (s, 1H, Ar-H), 8.30 (d, 1H, Ar-H), 7.83 (d, 1H, Ar-H), 7.74 (d, 1H, Ar-H), 7.63 (s, 1H, Ar-H), 7.57 (s, 1H, Ar-H), 7.53 (d, 1H, Ar-H). MALDI-TOF-MS (*m*/*z*): calcd. 355.336 for C<sub>18</sub>H<sub>8</sub>F<sub>3</sub>N<sub>3</sub>S; found 355.341 [M]<sup>+</sup>.

### 2. 2. 2. General Synthesis Procedure for Phthalocyanine Derivatives (TiPc1-3)

A mixture of the related phthalonitrile derivative (1–3) (0.28 mmol), DBU (0.50 mmol, 0.3 mL), and Ti(O-Bu)<sub>4</sub> (0.6 mmol, 0.2 ml) in *n*-pentanol (3 mL) were stirred at 110<sup>0</sup>C under Ar for 12 h. The dark-green product was cooled to room temperature, precipitated by the addition of *n*-hexane, collected by using a centrifuge and then washed with n-hexane, methanol and ethanol. The dark-green product was purified performing column chromatography on silica gel with CHCl<sub>3</sub> as the eluent. The pure compounds were obtained as a mixture of four structural isomers. The obtained pure dark green crystal products (TiPc1-3) were characterized by applying different spectroscopic techniques (FT-IR, <sup>1</sup>H-NMR and MS spectroscopy).

#### {2,(3) 9(10),16(17),23(24)-tetrakis-(4-(7-methoxyquinolin-4-yl)oxy)- phthalocyaninato}oxo-titanium (IV) (TiPc1)

Yield: 0.025 g (44%). FT-IR (ATR) (cm<sup>-1</sup>): 3070 (Ar. C–H), 2930-2928 (Aliph. C–H), 1272-1018 (C–O–C), 923 (Ti=O).  $^{1}$ H NMR (500 MHz, Chloroformd) ( $\delta$ : ppm): 8.88-8.40 (b, 13H, Ar-H), 8.26-8.08 (b, 6H, Ar-H), 8.00-7.77 (b, 5H, Ar-H), 7.60-7.48 (b, 2H, Ar-H), 7.00-6.74 (b, 6H, Ar-H), 4.07 (s, 12H). MALDI-TOF-MS (m/z): calcd.1269.061 for  $C_{72}H_{44}N_{12}O_{9}Ti$ ; found 1269.767 [M] $^{+}$ .

### {2,(3)9(10),16(17),23(24)-tetrakis-(4-(quinolin-2-ylthio))-phthalocyaninato}oxo-titanium(IV) (TiPc2)

Yield: 0.05 g (58%). FT-IR (ATR) (cm<sup>-1</sup>): 3070 (Ar. C-H), 1497-1336 (C-S-C), 940 (Ti=O). <sup>1</sup>H NMR (500

MHz, Chloroform*d*) (δ: ppm): 9.73-9.12 (b, 8H, Ar-H), 8.47-8.19 (b, 2H, Ar-H), 8.13-7.32 (b, 26H, Ar-H). MAL-DI-TOF-MS (m/z): calcd. 1212.220 for  $C_{72}H_{44}N_{12}O_9Ti$ ; found 1212.570 [M]<sup>+</sup>.

## {2,(3)9(10),16(17),23(24)-tetrakis-(4-(7-(trifluorome-thyl)quinolin-4-yl)thio))-phthalocyaninato oxo-titani-um(IV) (TiPc3)

Yield: 0.025 g (50%). FT-IR (ATR) (cm $^{-1}$ ): 3050 (Ar. C–H), 1368–1284 (C–S–C), 894 (Ti=O).  $^{1}$ H NMR (500 MHz, Chloroformd) (δ: ppm): 9.00-8.60 (b, 10H, Ar-H), 8.65-8.17 (b, 12H, Ar-H), 7.95-7.69 (b, 3H, Ar-H), 7.76–7.42 (b, 6H, Ar-H), 7.06 (s, 12H) MALDI-TOF-MS (m/z): calcd. 1485.212 for  $C_{72}H_{32}F_{12}N_{12}OS_4Ti$ ; found 1421.762 [M-(CF<sub>3</sub>)+5H] $^{+}$ .

#### 2. 3. Computational Details

Density Functional Theory (DFT) and Time Dependent- Density Functional Theory (TD-DFT) methods are used for throught of the study with Gaussian09 software.<sup>26</sup> Conformational analyses and geometry optimizations of all the structures are performed to determine the most stable structures. Geometry optimizations of the most stable conformers are done using B3LYP/LANL2DZ basis set. Single point energies are calculated using Becke's three-parameter Lee-Yang-Parr functional (B3LYP) effective core potential calculation where 6-31g(d) basis set for C, H, N, O, S, F and LANL2DZ basis set are used for Ti. Stationary points verification of the molecular structures as a global minimum are performed by frequency calculation with no imaginary frequencies. The <sup>1</sup>H NMR calculations are performed by gauge-independent atomic orbital (GIAO) approach. The Frontier Molecular Orbital (FMO) visualitions and Molecular Electrostatic potential (MEP) surfaces are also obtained with mentioned method by using Gausview.<sup>27</sup>

Conductor like Polarizable Continuum Model (CPCM), an implicit solvent model, is used with the intention of understanding solvent effect. Solvents are DMSO, DMF, THF, CHCl<sub>3</sub> with the dielectric constants values 46.83, 37.22, 7.43 and 4.71 respectively.<sup>28</sup>

The global reactivity indices of molecules are calculated with using of Koopman's Theorem. With this theorem it is stated that ionization potential and electron affinity are related to negative values of energies of Highest Occupied Molecular Orbital ( $E_{HOMO}$ ) and Lowest Unoccupied Moldecular Orbital ( $E_{LUMO}$ ) respectively. Then, chemical potential ( $\mu$ ), hardness ( $\eta$ ), electrophilicity index ( $\omega$ ) and softness (S) are calculated with equations 1–4.<sup>29</sup>

$$\mu = \frac{E_{LUMO} - E_{HOMO}}{2} \tag{1}$$

$$\eta = \frac{E_{LUMO} + E_{HOMO}}{2} \tag{2}$$

$$\omega = \frac{\mu^2}{2 \times n} \tag{3}$$

$$S = \frac{1}{2 \times \eta} \tag{4}$$

The local reactivity indices, fukui functions are obtained by using finite diffrence method which proposed Yang and Mortier. The equations that given below are fukui functions for nucleophilic  $(f_{(r)}^+)$ , electrophilic  $(f_{(r)}^-)$  and radicalic  $(f_{(r)}^0)$  attack.<sup>30,31</sup>

$$f_{(r)}^+ = p_{N+1}(r) - p_N(r) \tag{5}$$

$$f_{(r)}^- = p_N(r) - p_{N-1}(r)$$
 (6)

$$f_{(r)}^{0} = \frac{p_{N+1}(r) - p_{N-1}(r)}{2} = \frac{f_{(r)}^{\dagger} - f_{(r)}^{-}}{2}$$
 (7)

In these equations  $p_N(r)$ ,  $p_{N+1}(r)$ ,  $p_{N-1}(r)$  are the calculated electron density of neutral, anionic and cationic molecule by using Mulliken Population Analysis. Local softness values are calculated by using the values of fukui functions as given below.<sup>31</sup>

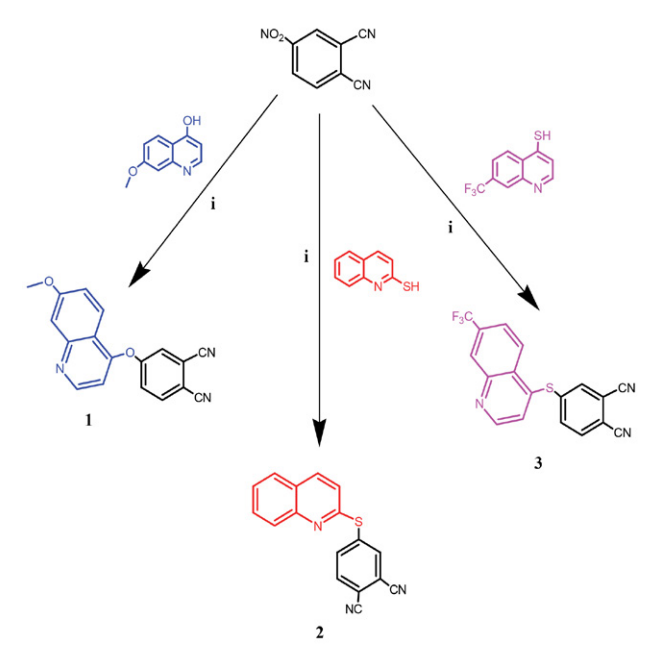
$$S_{(r)} = S \times f_{(r)} \tag{8}$$

#### 3. Results and Discussion

#### 3. 1. Synthesis and Characterization

As shown in Scheme 1, by adding 4-nitrophthalonitrile to 7-methoxyquinolin-4-ol, quinoline-2-thiol, and 7-(trifluoromethyl)quinoline-4-thiol, phthalonitrile derivatives (1, 2 and 3) are achieved by the nucleophilic aromatic substitution reaction in anhydrous  $K_2CO_3$  and dry DMF medium.

The pure product resulting from the reaction to obtain tetra-substituted Pc is predicted to be a mixture of



**Scheme 1.** Synthesis pathway of phthalonitrile derivatives (1, 2 and 3). Reaction conditions: i) i)  $K_2CO_3$ , DMF, rt, 24 h.

$$R_{1} = \bigcap_{N \to \infty} CN \qquad i \qquad R_{1} = \bigcap_{N \to \infty} CN \qquad i \qquad R_{2} = \bigcap_{N \to \infty} R_{2} \qquad R_{3} = \bigcap_{N \to \infty} R_{2} \qquad R_{3} = \bigcap_{N \to \infty} R_{3} = \bigcap_{N \to \infty} R_{2} = \bigcap_{N \to \infty} R_{3} = \bigcap_{N$$

Scheme 2. The synthesis pathways of Ti(IV) phthalocyanines (TiPc1-3) used phthalonitrile derivatives (1-3). Reaction conditions: i) Ti(OBu)<sub>4</sub>, *n*-pentanol, 110 °C, 12 h.

four structural isomers of this tetra-substituted phthalocyanine, differing in symmetry. 32-35

Scheme 2 presents the synthesis route of the pure products **TiPc1**, **TiPc2**, and **TiPc3**, each obtained as a mixture of its four structural isomers via cyclotetramerization of compounds the compounds 4-(7-methoxyquinolin-4-yl)oxy) phthalonitrile (1), 4-(quinolin-2-ylthio)phthalonitrile (2) and 4-((7-(trifluoromethyl)quinolin-4-yl)thio)phthalonitrile (3). As seen in Scheme 2, the reaction of starting compounds 1, 2 and 3 with Ti(OBu)<sub>4</sub> in the presence of DBU in *n*-pentanol produced **TiPc1**, **TiPc2** and **TiPc3**. The main synthesis products peripherally tetra-substituted **TiPc1**, **TiPc2** and **TiPc3** were isolated from the crude product mixture by column chromatography using CHCl<sub>3</sub> as the eluent.

**TiPc1**, **TiPc2** and **TiPc3** are characterized by FT-IR, <sup>1</sup>H-NMR, MALDI-TOF and UV-Vis spectroscopic meth-

ods. The obtained results with these techniques are compatible with the expected structures for all prepared Pcs.

Experimental and calculated results of the most characteristic corresponding assignments of compounds are listed in Table 1. The given FT-IR values, those in parentheses show the calculated results. The characteristic C≡N vibrations for phthalonitriles 1, 2, and 3 are observed at 2239 cm<sup>-1</sup>, 2229 cm<sup>-1</sup>, and 2235 cm<sup>-1</sup> respectively. When the FT-IR spectrum of the **TiPc1** compound is examined (Figure S1), the characteristic C≡N vibration observed in phthalonitrile compounds disappears and peaks belonging to aliphatic C-H groups appear in the range of 2928-2930 cm<sup>-1</sup> (approximately 2911.91 cm<sup>-1</sup>). C−O−C vibration is observed at 1018-1227 cm<sup>-1</sup> (approximately 1387.38 cm<sup>-1</sup>) for the **TiPc1** compound. In addition, the formation of the characteristic Ti-O stretch peak around 923 cm<sup>-1</sup>

(1031.57 cm<sup>-1</sup>), as well as the sharp peaks observed in the 555–630 cm<sup>-1</sup> range are indicative of **TiPc1** formation. In the FT-IR spectra of **TiPc2** and **TiPc3** (Figure S1), the vibrations of the C–S–C groups at 1497–1336 cm<sup>-1</sup> (1355.01 cm<sup>-1</sup>) for **TiPc2** and for **TiPc3** at 1368–1284 cm<sup>-1</sup> (1254.81 cm<sup>-1</sup>).<sup>20</sup> The vibrations of the characteristic C-F bond for **TiPc2** are determined at 1150–1115 cm<sup>-1</sup> (1173.12 cm<sup>-1</sup>). Experimental and calculated frequencies are in good agreement with each other and the literature.<sup>36</sup> The sharp peaks of characteristic Ti-O stretching are observed around 940 cm<sup>-1</sup> and 894 cm<sup>-1</sup> for **TiPc2** and **TiPc3**, respectively. The corresponding Ti-O frequencies in the DFT calculations are to be 1032.22 cm<sup>-1</sup> and 1034.75 cm<sup>-1</sup> for **TiPc2** and **TiPc3** respectively. These results are indicative of the formation of **TiPc2** and **TiPc3**.

In this study, the unharmonic corrections to calculated IR results are done by multiplying the calculated wave number value with scaling factors 0.983 and 0.958 for be-

In addition to <sup>1</sup>H NMR spectrum results, the MAL-DI-TOF MS data for the phthalonitrile derivatives (**1**, **2**, and **3**) and their titanium (IV) phthalocyanine derivatives (**TiPc1**, **TiPc2**, and **TiPc3**) are available for the formulations given. The molecular ion peaks of synthesized compounds show parent ions at m/z: 301.687 as [M]<sup>+</sup> for **1**, 286.00 [M]<sup>+</sup> for **2**, 355.341[M]<sup>+</sup> for **3**, 1269.767 [M+H]<sup>+</sup> for **TiPc1**, 1212.570 [M]<sup>+</sup> for **TiPc2**, 1661.878 [M+5K+6H]<sup>+</sup> for **TiPc3**, respectively The molecular ion peak values of the fragmentation products of the obtained complexes are also indicated in the supplementary file (Fig. S4a-f).

### 3. 2. Ground State Electronic Absorption Spectras

The phthalocyanine macrocyclic system is characterized by quite strong absorption bands the Soret and Q bands corresponding to the  $\pi \rightarrow \pi^*$  transitions. The former

	TiPc1		TiPe	c2	TiPc3		
	Exp.	Calc.	Exp.	Calc.	Exp.	Calc.	
v <sub>stretchingC-H(aliphatic)</sub>	2930-2928	2911.91	=	_	_	_	
v <sub>stretchingC-H(aromatic)</sub>	3070	3087.44	3070	3059.36	3050	3106.59	
$\delta_{bendingC-O-C}$	1227-1018	1387.38	_	_	_	_	
$v_{\text{stretchingTi-O}}$	923	1031.57	940	1032.22	894	1034.75	
$\delta_{bendingC-S-C}$	_	_	1497-1336	1355.01	1368-1284	1254.81	
$v_{\text{stretchingC-F}}$	_	_	_	_	1150-1115	1173.12	

**Table 1.** Comparison of experimental and calculated FTIR results (in cm<sup>-1</sup>).

low and greater than 1700 cm<sup>-1,37</sup> All the stretching and bending vibrations are anticipated range and Table 1 demonstrates the agreement between experimental and calculated wavenumbers. The convergence of experimental and theoretical results reinforces the reliability of the identification of compounds.

The <sup>1</sup>H NMR results provide acceptable data about the suggested configurations of the designed complexes. <sup>1</sup>H NMR results together with computationally obtained ones are given in the supplementary material with Table S1. The <sup>1</sup>H-NMR spectrums of the phthalonitrile compounds 1, 2, and 3 indicate signals with  $\delta$  ranging from 3.95 to 9.91 (for 1, integrating for 8H aromatic-CH protons and 3H aliphatic-CH<sub>3</sub> protons), 7.20 to 8.18 (for 2, integrating for 9H aromatic-CH protons), 7.0 to 8.5 (for 3, integrating for 8H aromatic-CH protons) as expected (Fig. S2a-c). The signals with integrating for 12H aliphatic-CH<sub>3</sub> and 32H aromatic-CH protons of TiPc1 are observed at 3.83 ppm and 6.95-9.06 ppm (Fig. S3a-c), respectively and these results indicate the formation of this complex. In the <sup>1</sup>H NMR spectrum of **TiPc2** and **TiPc3**, the signals of the aromatic-CH are detected at the range of 9.73-7.32 ppm (integrating for 36H) and 9.10-7.18 ppm (integrating for 32H), respectively, and confirming the formation of TiPc2 and TiPc3 (Fig. S3).

is at 300-350 nm and the latter is observed in the visible region at 600-700 nm in the UV-Vis spectrum.<sup>38</sup> With the central metal ion effect, metallophthalocyanines with D4h symmetry give a single Q band in the visible region, while non-metallic phthalocyanines with D2h symmetry show two bands with equal intensity in the same range in the visible region. The ground state electronic absorption spectra of Ti(IV) phthalocyanines for DMSO, DMF, THF, and chloroform solutions are recorded and the characteristic Soret and single Q bands of newly synthesized phthalocyanines TiPc1, TiPc2 and TiPc3 are detected in their electronic spectra. Hence, the obtained results are one of the principal pieces of evidence for their formation. The obtained spectral datas confirm the structures of the targeted Pcs are convenient with the electronic absorption spectra of other MPcs.<sup>39</sup>

The electronic spectra of **TiPc1** bearing 4-(7-methoxyquinolin-4-yl)oxy) isoindole moieties (Fig. 1) shows the characteristic absorption bands at around 690, 694 and 697 nm for the Q band region which is characteristic of metallophthalocyanines in DMF, THF, and chloroform, respectively.<sup>20,39,40</sup> Although **TiPc1** has a high solubility in the previously mentioned organic solvents, its solubility in DMSO is very low, and no appreciable absorption spectrum is observed.

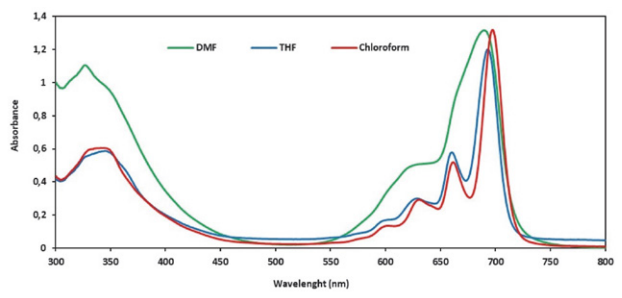
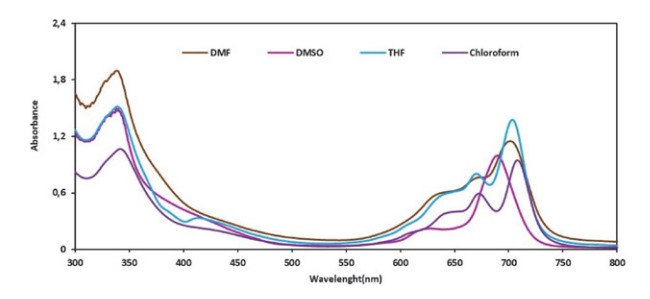


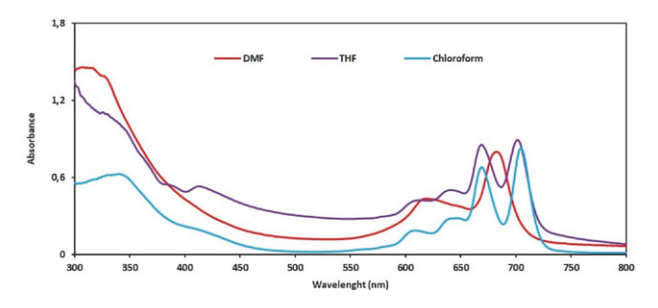
Figure 1. Electronic absorption spectrum of TiPc1 in DMF, THF and chloroform.

Fig. 2 presents the absorption spectra of **TiPc2** bearing 4-(quinolin-2-ylthio) isoindole moieties in the mentioned solvents. The Q band of **TiPc2** in DMSO, DMF, THF, and chloroform are observed at 689, 700, 703 ve 708 nm, respectively.



**Figure 2.** Electronic absorption spectrum of **TiPc2** in DMSO, DMF, THF and chloroform.

Fig. 3 shows the Q bands of **TiPc3** bearing 4-((7-(tri-fluoromethyl) quinoline-4-yl)thio) isoindole in DMF, THF, and chloroform. The solubility of **TiPc3** in the previously mentioned organic solvents is very high; however, its solubility in DMSO is very low, and an appreciable spectrum of absorption is not recorded. The Q band characteristic for metalized phthalocyanine is observed at 683 nm in DMF solution. The Q-bands of the obtained **TiPc3** are split into two components, Qx and Qy, which could result from the solvent effect decreasing symmetry.<sup>41</sup>



**Figure 3.** Electronic absorption spectrum of **TiPc3** in DMF, THF and chloroform.

#### 3. 3. TD-DFT Results and FMOs

TD-DFT calculations are used to interpret experimental results. The comparison of experimental UV-Vis results with TD-DFT ones is done and given in Table 2. It is understood that the resulting wavelengths correspond with experimentally obtained maximum absorption wavelengths ( $\lambda_{exp}$ ) results. The percentage of errors for calculations ranges between 1.44 % and 5.04 %. For TiPc2 compound the calculated (experimental) maximum wavelength value is 672.33 (708) nm for chloroform phase (Fig S5). The small discrepancies between the experimental and calculated are the results of environmental factors of experimental conditions and quantum mechanical effect in a chosen computational model.

All the Q absorption bands of newly synthesized compounds are red-shifted. Red shifted absorption is a needed property to use them effectively as photosensitizers and dye-sensitized solar cells. 18,19 Photochromic behavior that is seen in the absorption spectrums can lead to these compound's usage in photodynamic therapy. TiPc2 has the most red-shifted absorption peak. This result does not differ with the changing of solvents. Red-shift values of compounds differ from each other and differ with the changing of solvent medium. Thus, the polarity of the solvent, metal atom in the Pc ring, and substituent can affect the red-shifted wavelength absorption of the Q band as stated in the literature. 42 From Table 2, it is also understood that the dominant transition occurs from the Highest Occupied Molecular Orbital (HOMO) to the Lowest Unoccupied Molecular Orbital (LUMO) which is a  $\pi$ - $\pi$ \* transition. As seen in Table 2, the  $\pi$ - $\pi$ \* transition of molecules occurs with approximately the same energy (1.85 eV) in all solvents. However, only in TiPc1, the energy is 0.02 eV higher than in other solvents except THF. In all molecules, transitions from HOMO to LUMO occur with a probability of 96%.

The frontier molecular orbitals (HOMO, LUMO) structures and their energies are given in Fig. 4, Fig. S6-7 and Table S2. It is understood from Fig. 4 that HOMO orbitals are all  $\pi$  type orbitals and LUMO orbitals are  $\pi^*$  type orbitals. HOMO orbitals are mainly distributed at the Pc ring for TiPc1. For TiPc2, the HOMO orbital is mainly located at the metallic part of the compound. As seen from the molecular orbital structure of the compound TiPc3, electron-withdrawing fluorine atoms of substituent leads to changing of electrons location in the HOMO orbital. Unlike TiPc1 and TiPc2 compounds, the HOMO orbital of **TiPc3** is not located in the metal atom or Pc ring but is distributed from the Pc ring to the sulfur linkage of the substituent. This may be the result of the highly electronegative character of its substituent. Thus it is important to note that substitutions with different groups have contributed to Frontier Molecular Orbital electronic structures. LUMO orbitals are distributed all over the Pc ring and metal atoms in all three compounds. Except for the HOMO orbital of TiPc1 in DMSO, the HOMO and LUMO orbitals

Table 2. Calculated UV Results of Compounds.

	ΔE (eV)	λ (nm)	f	Transition	$\lambda_{exp}$ (nm)
DMSO					
TiPc1	1.87	663.64	0.66	HOMO→LUMO (96.34%)	_
TiPc2	1.84	672.63	0.62	HOMO→LUMO (96.74%)	689
TiPc3	1.84	672.67	0.64	HOMO→LUMO (96.59%)	_
DMF					
TiPc1	1.87	664.16	0.66	HOMO→LUMO (96.39%)	690
TiPc2	1.84	673.14	0.62	HOMO→LUMO (97.78%)	700
TiPc3	1.84	673.13	0.64	HOMO→LUMO (96.62%)	683
THF					
TiPc1	1.85	669.90	0.61	HOMO→LUMO (96.17%)	697
TiPc2	1.85	671.19	0.61	HOMO→LUMO (96.70%)	703
TiPc3	1.85	670.17	0.63	HOMO→LUMO (96.52%)	702
CHCl <sub>3</sub>					
TiPc1	1.87	663.88	0.66	HOMO→LUMO (96.17%)	694
TiPc2	1.84	672.33	0.63	HOMO→LUMO (96.80%)	708
TiPc3	1.85	671.52	0.65	HOMO→LUMO (96.62%)	707

of **TiPc1**, **TiPc2**, and **TiPc3** in DMF, THF, CHCl<sub>3</sub>, and vacuum are distributed on the metallic part or Pc ring of the compounds. The HOMO of **TiPc1** is located on the substituent part for the DMSO.

The energy values of HOMO and LUMO of compounds are given in Table S2. The negative energy values of the HOMO and LUMO of the compounds indicate the chemical stability of the compounds in both aprotic and

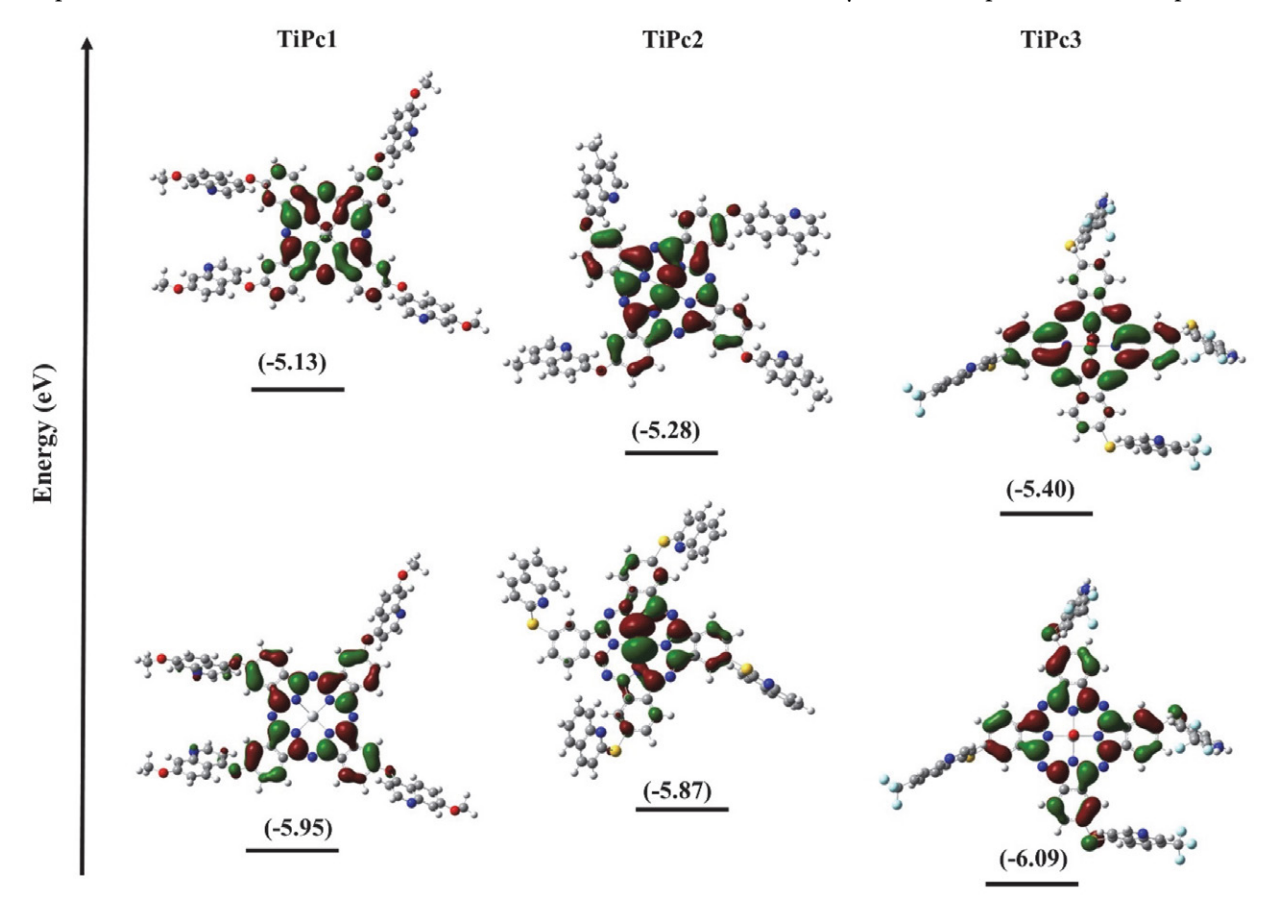


Figure 4. Frontier orbitals energies of TiPc1, TiPc2 and TiPc3 in CHCl<sub>3.</sub>

non-polar solvents. The lowest HOMO energy belongs to the **TiPc3** compound and its values are –6.21, –6.20, –6.06, –6.09, and –5.96 eV for DMSO, DMF, THF, chloroform, and vacuum, respectively. HOMO energy values of **TiPc3** are lower in aprotic solvents. Energies of LUMO orbitals are, –5.13 eV, –5.28 eV, and –5.40 eV for **TiPc1**, **TiPc2** and **TiPc3** for chloroform medium respectively. As seen in Fig. 4, the electron donor energy of **TiPc3** is smallest in chloroform (–6.09 eV). We can conclude that the solvent not only affects the structures of the boundary molecular orbitals, but also the energies.

For using a compound as a dye-sensitized solar cell some criteria like the red-shifted absorption spectrum and small  $\Delta E$  values (near 1.4 eV) are needed. 19,43 Light harvesting efficiency (*LHE*) is another important factor for examining a compound's optical usabilities as a dye-sensitized solar cell. High *LHE* values play a pivotal role in getting maximum photocurrent from a compound. 44,45 The excited state lifetime ( $\tau$ ) is another factor for getting high

charge transfer efficiency. When the excited state lifetime of a material increases, its optical stability as well as its charge transfer ability increases. LHE and the excited lifetime can be calculated as follows:<sup>44,46</sup>

$$LHE = 1 - 10^{-f} \tag{9}$$

$$\tau = \frac{1.499}{fE_{ex}^2} \tag{10}$$

In Eq. 9 and 10 f is the oscillator strength and  $E_{\rm ex}$  is excitation energy in cm<sup>-1</sup> unit. *LHE* and  $\tau$  values of the compounds are shown in Table 3. According to Table 3, the *LHE* and  $\tau$  values of all compounds are greater than 0.75 and 9.98 ns. So, **TiPc1**, **TiPc2** and **TiPc3** can absorb more photons from UV light. He highest *LHE* values of the compounds are in CHCl<sub>3</sub> solvent and the *LHE* order is **TiPc2** < **TiPc1**= **TiPc3**. It can be concluded that **TiPc1**, **TiPc2** and **TiPc3** are suitable compounds for dye-sensitized solar cell applications. With comparing literature de-

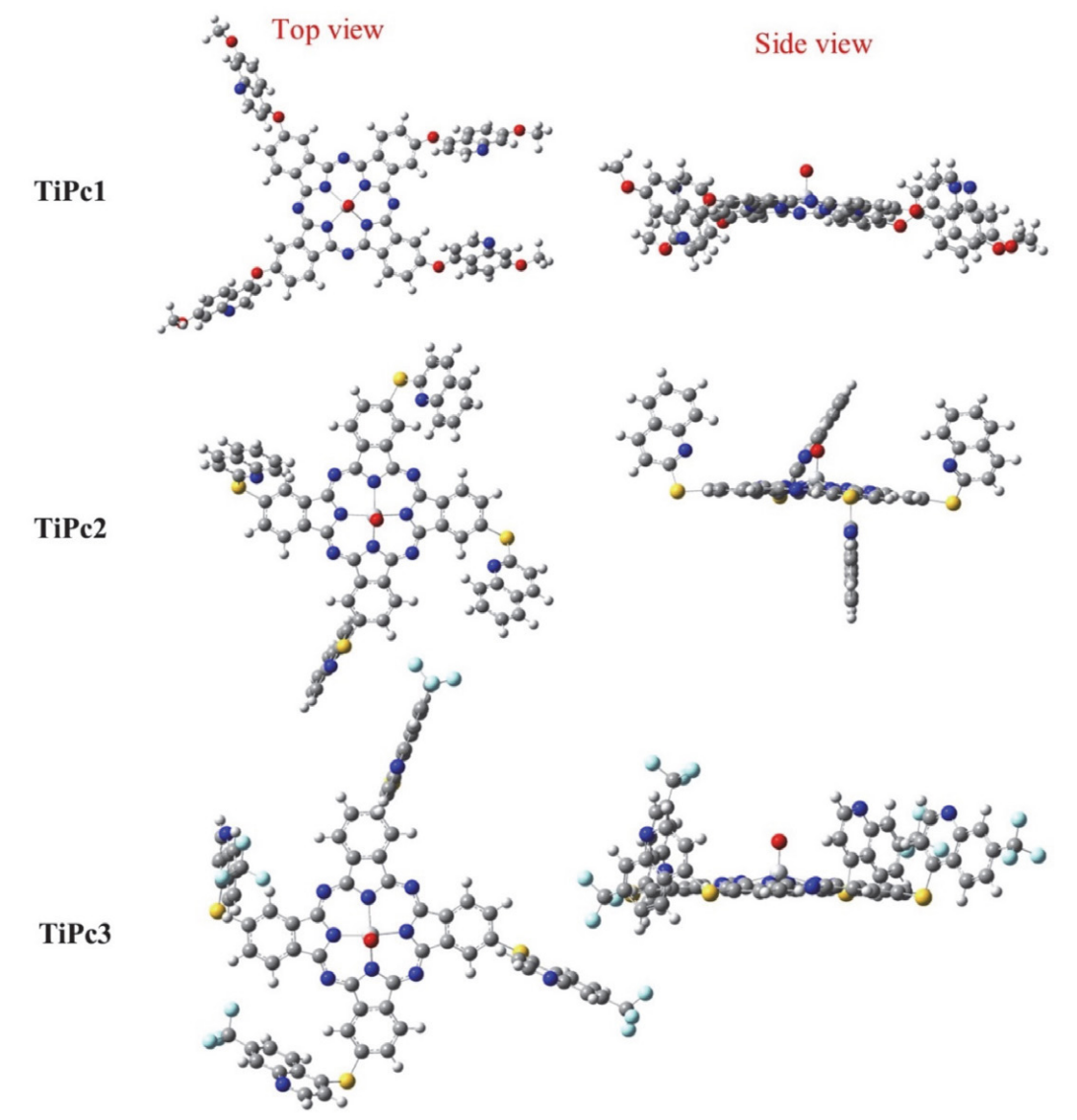


Figure 5. Optimized molecular geometries of TiPc1, TiPc2 and TiPc3.

signing Pc with the oxo-titanium moiety may be also suitable method for obtaining higher excited state lifetimes.<sup>44</sup>

**Table 3.** Calculated *LHE* and  $\tau$  values of **TiPc1**, **TiPc2** and **TiPc3**.

	TiPc1	LHE TiPc2	TiPc3	τ (ns) TiPc1 TiPc2 TiPc3
DMSO	0.78	0.76	0.77	9.98 10.98 10.63
DMF	0.78	0.76	0.77	9.98 10.98 10.63
THF	0.75	0.75	0.77	11.04 11.04 10.63
CHCl <sub>3</sub>	0.78	0.77	0.78	9.98 10.80 10.36

#### 3. 4. Calculated Electronic Properties

To examine the effects of the substituent groups on the molecular structure and reactivity in TiPc1, TiPc2 and TiPc3 compounds, calculations are also made for TiPc0, which does not contain substituents. The optimum geometric structures and geometric parameters of the compounds are given in Fig. 5 and Supplementary Material. As expected, the geometric parameters are very close to each other due to the planarity in the center of the complexes.

When the optimized compounds are viewed from the top position, it is seen that the peripherally substituted parts of the synthesized compounds disrupt the planarity of the compounds (Figure 5). 4-((7-methoxyquinolin-4-yl) oxy), 4-(quinolin-2-ylthio) and 4-((7-(trifluoromehyl) quinolin-4-yl)thio) peripherally substituted parts of oxotitanium phthalocyanines oriantates out of the plane when viewed from the side position. This orientation in the compund causes the dipole moment and solubility of the compound to increase. Thus, this result also verifies the experimental part result for the solubility ability of compounds in the THF, DMF and CHCl<sub>3</sub>.

Geometric parameters of the compounds (Table S3) are also given. The bond lengths of Ti and pyrrole nitrogen are 2.08, 2.07, 2.08, and 2.08 Å for **TiPc0, TiPc1, TiPc2,** and **TiPc3**, respectively. Substituents containing oxygen bridge affects this bond length, but substituents with sulfur bridges do not affect this bond length. The bond length of Ti and meta nitrogen atoms is 3.47 Å for all compounds. The angle between the substituents and Pc ring is 122.02<sup>0</sup>, 102.71<sup>0</sup>, and 102.52<sup>0</sup> for **TiPc1, TiPc2,** and **TiPc3** respectively.

Electronic energies, dipole moments, energy differences of FMOs, and global reactivity indices are given in Table 4. As seen in Table 4, TiPc3 is the compound with the smallest electronic energy and therefore the most stable in all solvents. The order of stability decreases to TiPc3 < TiPc2 < TiPc1 < TiPc0. The electronegative fluorine

**Table 4.** Calculated energy (Energy (E), energy difference of the frontier orbital ( $\Delta E$ )) and reactivity parameters (hardness ( $\eta$ ), chemical potential ( $\mu$ ), electrophilic index ( $\omega$ ), and softness (S)) for complexes .

	E (Hartree)	D (Debye)	ΔE (eV)	η (eV)	μ (eV)	ω (eV)	S (eV)
DMSO							
TiPc0	-2592.01	4.85	2.05	1.03	-4.28	8.94	0.49
TiPc1	-4357.99	13.97	0.68	0.34	-5.73	48.15	1.47
TiPc2	-5191.73	14.10	0.78	0.39	-5.79	42.95	1.28
TiPc3	- 6539.90	25.50	0.80	0.40	-5.87	43.14	1.25
DMF							
TiPc0	-2592.01	4.84	2.05	1.03	-4.28	8.93	0.49
TiPc1	-4357.99	13.91	0.68	0.34	-5.72	47.93	1.46
TiPc2	-5191.73	14.05	0.77	0.38	-5.78	43.46	1.30
TiPc3	-6539.90	25.42	0.79	0.39	-5.86	43.52	1.27
THF							
TiPc0	-2592.20	4.63	2.06	1.03	-4.25	8.78	0.49
TiPc1	-4357.97	12.54	0.69	0.35	-5.66	46.40	1.45
TiPc2	-5191.71	12.96	0.65	0.32	-5.62	48.67	1.54
TiPc3	-6539.89	23.92	0.70	0.35	-5.78	47.52	1.42
CHCl <sub>3</sub>							
TiPc0	-2592.00	4.48	2.06	1.03	-4.23	8.69	0.48
TiPc1	-4357.96	11.61	0.67	0.34	-5.61	46.86	1.49
TiPc2	-5191.70	12.15	0.59	0.29	-5.58	52.82	1.70
TiPc3	-6539.87	22.91	0.68	0.34	-5.75	48.41	1.46
Vacuum	1						
TiPc0	-2591.99	3.43	2.09	1.04	-4.09	8.00	0.48
TiPc1	-4357.88	6.72	0.91	0.46	-5.22	29.88	1.10
TiPc2	-5191.63	7.32	0.62	0.31	-5.17	42.85	1.60
TiPc3	-6539.80	16.52	0.70	0.35	-5.72	47.03	1.44

atom in the **TiPc3** structure may lead to the stabilization of the compound. The energies of compounds are lower in solvents than in vacuum.

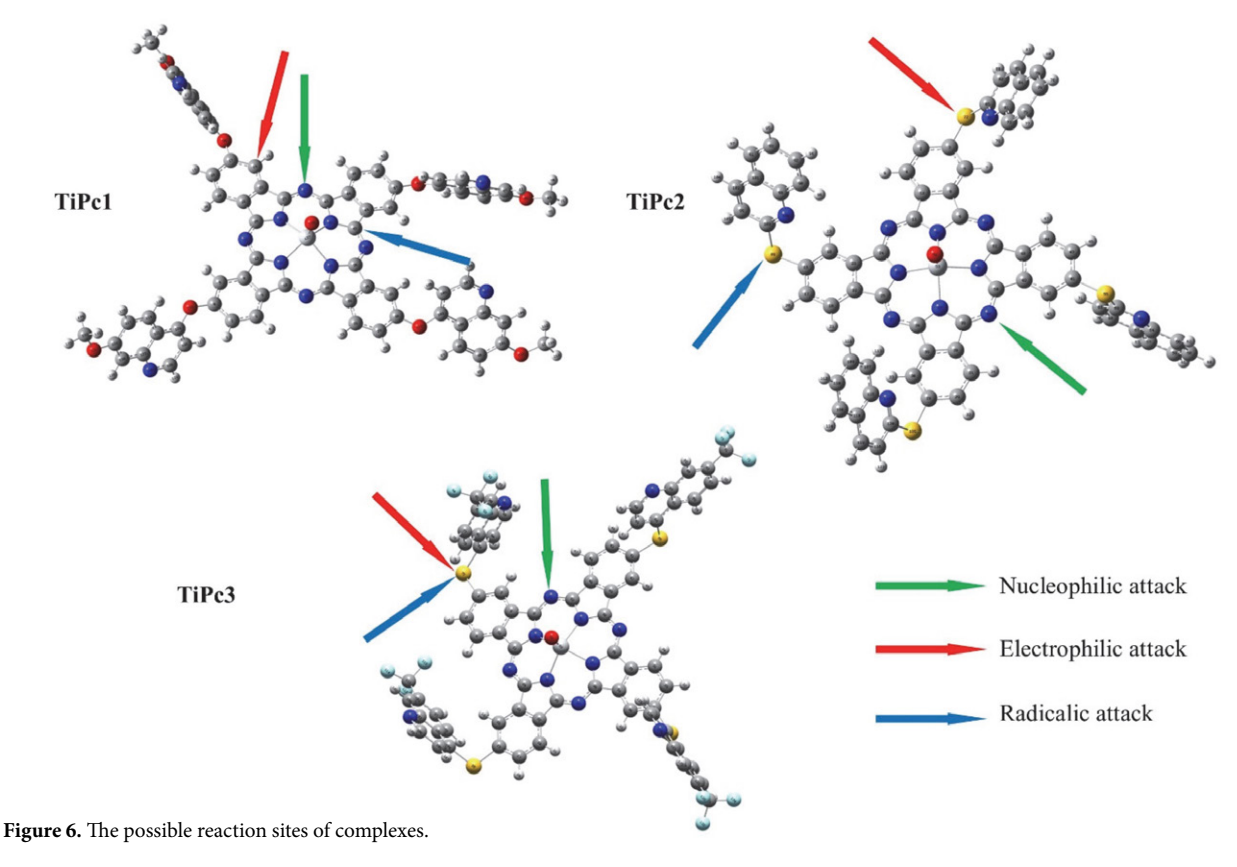
As seen in Table 4, the dipole moments of the compounds are lower in vacuum. Dipole moment values of compounds are related to their molecular structures, as mentioned before. Generally, the large dipole moment causes the molecule to self-assemble<sup>47</sup> **TiPc3** contains more electronegative atoms than other compounds. Therefore, this may be the reason why **TiPc3**, which has the highest dipole moment among all phases, is also the most photochemically stable character. A high dipole moment is a desired feature in the drug distribution process.<sup>48</sup> Therefore, **TiPc3** may be a suitable drug candidate. These results show that substituents of molecular structures have an important effect on the electronic nature. Therefore, theoretical calculations are essential to obtain substituent effects on molecular properties.

The energy difference of the frontier orbital ( $\Delta E$ ) determines the reactivity of a compound. The small energy gap indicates that the molecule is more reagent.<sup>49</sup> As seen in Table 4, the reactivity of the compounds changes as the solvent changes. The molecular reactivity of the compounds is highest in non-polar chloroform. A high electron population in the conductive bond is a desired feature in the drug delivery system. Decreasing the energy difference between the boundary orbitals increases the electron population in the conductive bond.<sup>50</sup> As seen from the  $\Delta E$  values s in Table 4, **TiPc0** has the lowest reactivity among

all compounds. Compared to **TiPc0**, it appears that **TiPc1**, **TiPc2** and **TiPc3** are candidates for drug delivery. This shows that adding new substituents to the molecular structure of Pcs increases their reactive properties.

Hardness is an important global reactivity indice to understand the chemical stability of compounds. While the **TiPc1** compound is the most reactive compound in DMSO and DMF with the smallest hardness value of 0.34 eV, **TiPc0** is the most stable in vacuum with the highest hardness value of 0.46 eV. In chloroform, the chemical potential value (-5.75 eV) of **TiPc3** is the smallest while the chemical potential value (-4.23 eV) of **TiPc0** is the highest. The electrophilic index value of **TiPc0** is smaller than other compounds in all mediums. As the softness has an inverse relationship with hardness, it can be deduced from Table 4 that the softness values of **TiPc0** and **TiPc3** are the smallest ones in DMSO and DMF and vice versa with hardness results.

Thermodynamic parameters of the compounds are given in Table S4. Heat capacity, entropy, enthalpy, and Gibbs free energy calculations are conducted at 298.15 K and 1 atm. As seen from the table values, the substituent also affects the thermodynamic properties of the compounds. The heat capacity of **TiPc0** is 118.46 cal.mol<sup>-1</sup>K<sup>-1</sup> which is smaller than **TiPc1** (171.52 cal.mol<sup>-1</sup>K<sup>-1</sup>), **TiPc2** (141.33 cal.mol<sup>-1</sup>K<sup>-1</sup>) and **TiPc3** (194.38 cal.mol<sup>-1</sup>K<sup>-1</sup>) respectively. It is generally understood that the reactivity of Pcs can be regulated as a function of the electronic character of the ring, substituents, and solvent.



Aydogdu et al.: Synthesis, Characterization and DFT Study of Ti(IV) ...

### 3. 5. Mulliken Charges And Local Reactivity Indices

The Mulliken charges are essential for understanding the properties of compounds.<sup>21</sup> The Mulliken charges of **TiPc1**, **TiPc2**, and **TiPc3** are listed in the supplementary material (Table S5-7).

Titanium atoms of TiPc1, TiPc2, and TiPc3 are the most positively charged atom (1.17) for all compounds. In the TiPc1 structure, 19 C is the most negatively charged atom (-0.56). The phenyl carbon to which the substituent is connected to the ligand by an oxygen bridge is more positively charged than the other carbon atoms in the ring. Due to the electronegative character of the oxygen atom, the hydrogen atoms of methoxy groups are more positively charged than other hydrogen atoms. Meta nitrogen atoms are positively charged. The most negatively charged atom in TiPc2 is the 25 N atom in the pyrrole ring with a value of -0.49. In this compound, the sulfur bridge atoms have positive charges. In the TiPc3 compound, the sulfur bridge atoms are positively charged. The most negatively charged atom of TiPc3 is the pyrrole nitrogen atom (38 N) and its Mulliken charge is -0.49. As a result of the electronegativity of the fluoride atoms in TiPc3, the positive charge on the carbon atoms in the trifluoromethyl groups decreases.

The local reactivity indices are important to determine suitable sites of compounds for nucleophilic, electro-

philic, and radicalic attacks. With the help of these indices, possible reaction mechanisms of compounds can be predicted.<sup>51</sup> Getting information about the nucleophilic and electrophilic regions is also important for complex and protein interactions.<sup>21</sup> Fig. 6 and Table S8-10 provide information on the results of the local reactivity indices.

By examining the values of local reactivity descriptors, it is clear that meta nitrogen atoms (27 N, 40 N, 14 N) of all compounds (TiPc1, TiPc2, TiPc3) are suitable sites for nucleophilic attack. The electrophilic attack regions of the compounds are 19 C, 72 S, and 75 S atoms of TiPc1, TiPc2, and TiPc3 respectively. The carbon atom of the benzene ring, and bridge sulfur atoms of compounds attract to electrophilic chemicals. It is understood that changing the bridging atom of substituent groups affects the reactivity. The sulfur atom bridge is an important reaction site for TiPc2 and TiPc3 in comparison with the oxygen bridge in TiPc1. The radical attack sites of TiPc1, TiPc2, and TiPc3 are 41 C, 89 S, and 75 S atoms of the compounds, respectively. In general, bridge atoms and meta-nitrogen atoms of compounds are suitable sites for different types of reactants.

#### 3. 6. Molecular Electrostatic Potential

The Molecular Electrostatic Potential (MEP) surface is a pictorial demonstration of the distribution of

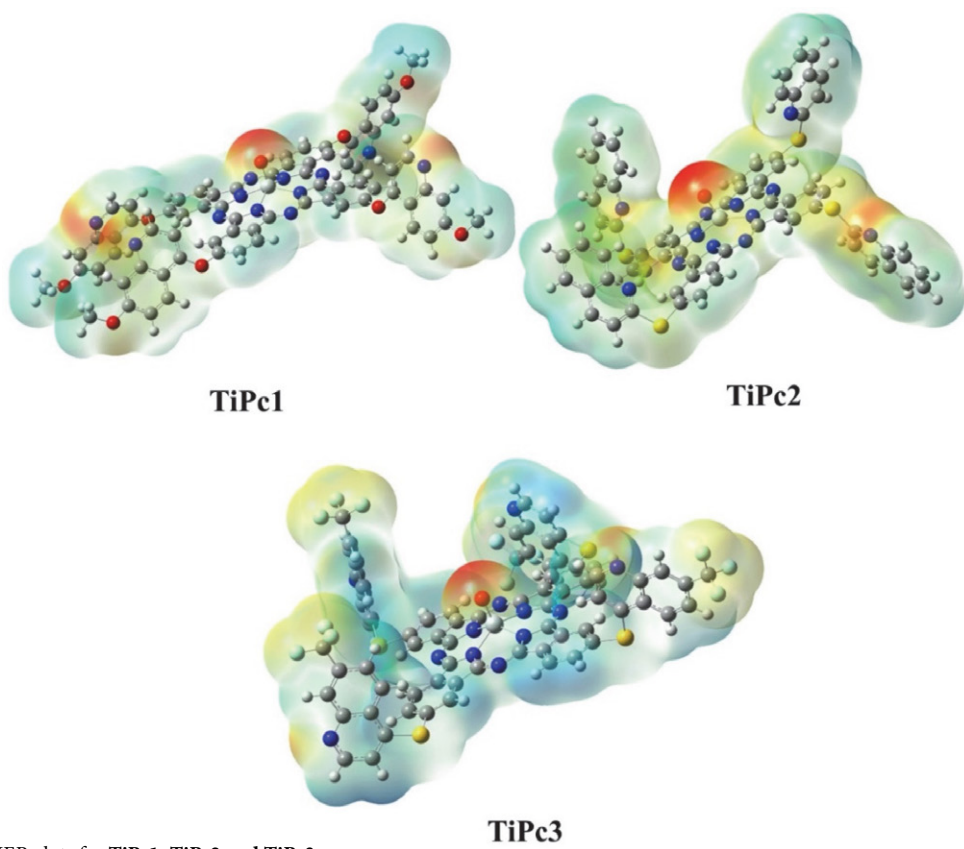


Figure 7. The MEP plots for TiPc1, TiPc2 and TiPc3.

electrons on the molecular structure. These surfaces are mainly used for determining the reactive sites of compounds. On these surfaces, the blue color regions represent the electron-deficient areas, while the red color regions represent electron-abundant areas.<sup>49</sup> The MEP surfaces are simulated with the B3LYP method and given in Fig. 7.

As illustrated in Fig 7 the most negative parts of all compounds are over the oxygen atom of the oxotitanium part, while the most positive parts of compounds are titanium atoms and hydrogen atoms. As can be observed, there are also some negative areas on the substituent parts of compounds, such as fluoride and nitrogen atoms, indicating that substituent groups are affecting the electronic distribution of compounds. As seen on the MEP surfaces, TiPc3 has more negative parts than other compounds. This is because TiPc3 has fluoride atoms in its molecular structure.

#### 4. Conclusions

In this study, new peripherally substituted oxo-titanium phthalocyanines (TiPc1, TiPc2 and TiPc3) containing three different substituents were synthesized. Characterization of all compounds by spectroscopic methods (FT-IR, <sup>1</sup>H-NMR, UV/Vis, and mass) was examined and their electronic properties were calculated by quantum chemical methods. The results of experimental and quantum chemical calculations are consistent with each other. It has been found that the main electronic transition in molecules occurs between HOMO and LUMO orbitals. The electron distributions in these orbitals are affected by the electron-withdrawing properties of the substigroups. Experimentally, the Q-band unsubstituted Ti(IV)Pc to the red shifted after the addition of the substituent in all solvents, and this was confirmed by the calculation results. Quantum chemical calculation results show that the electronegativity of the substituents leads to the formation of more stable compounds. In addition, changing the solvent also affects the electronic structure, energies, and reactivity. The effect of substituents on solubility was investigated in DMSO, DMF, THF and CHCl<sub>3</sub>. Experimental and computational results showed that adding substituents to Ti(IV)Pc increased the solubility of the compounds in THF, DMF, and CHCl<sub>3</sub>. In non-polar chloroform, compounds become more reactive. Electrophilic, nucleophilic, and radical attack sites of Pcs were also determined with the calculated local reactivity indices. In the complexes, the meta nitrogen atoms and the sulfur bridges connected by the substituent to the ligand are reactive centers where reactions can take place. As a result, it can be said that the synthesized compounds are suitable for dye-sensitized solar cells, photodynamic therapy, and drug delivery applications.

#### Declaration of competing interest

Authors declare that they have no conflicts of interest.

#### Acknowledgements

This study is supported by Yildiz Technical University Research Coordination with Project Number: FBA-2020-4025.

#### Supplementary material

Supplementary material associated with this article can be found at  $\dots$ 

#### 5. References

- J. D. Spikes, *Photochem. Photobiol.* **1986**, *43*, 691–699.
   **DOI:**10.1111/j.1751-1097.1986.tb05648.x
- A. Q. Alosabi, A. A. Al-Muntaser, M. M. El-Nahass, A. H. Oraby, *Opt. Laser Technol.* 2022, *155*, 108372.
   DOI:10.1016/j.optlastec.2022.108372
- F. Ayaz, D. Yetkin, A. Yüzer, K. Demircioğlu, M. Ince, *Photo-diagnosis Photodyn. Ther.* 2022, 39, 103035.
   DOI:10.1016/j.pdpdt.2022.103035
- 4. I. Paramio, T. Torres, G. de la Torre, *Org. Chem. Front.* **2023**, *11*, 60–66. **DOI**:10.1039/D3QO01630G
- R. Ağcaabat, C. Bilen Şentürk, Z. Odabaş, *Polyhedron* 2022, 222, 115929. DOI:10.1016/j.poly.2022.115929
- Ö. Güngör, Altinbaş G. Özpinar, M. Durmuş, V. Ahsen, *Dalton Trans.* 2016, 45, 7634–7641. DOI:10.1039/C6DT00874G
- S. Aydogdu, G. Yaşa-Atmaca, A. Erdoğmuş, A. Hatipoglu, Polyhedron, 2024, 256, 116989.
   DOI:10.1016/j.poly.2024.116989
- 8. I. Gusev, M. Ferreira, M. Krzywiecki, A. Przybyła, S. Pluczyk-Małek, D. Nastula, A. Duda, K. Nastula, K. Erfurt, P. Data, A. Blacha-Grzechnik, *Dyes and Pigm.* **2023**, *214*, 111217.

**DOI:**10.1016/j.dyepig.2023.111217

- X. Zhao, Q. Wang, X. Jia, J. Xue, J. A Chen, *Dyes and Pigm*.
   2022, 207, 110717. DOI:10.1016/j.dyepig.2022.110717
- S. Bhattacharya, G. Reddy, S. Paul, S. S. Hossain, S. S. Kumar Raavi, L. Giribabu, A. Samanta, V. R. Soma, *Dyes and Pigm*. 2021, 184, 108791. DOI:10.1016/j.dyepig.2020.108791
- M. Halaskova, A. Rahali, V. Almeida-Marrero, M. Machacek, R. Kucera, B. Jamoussi, T. Torres, V. Novakova, A. De La Escosura, P. Zimcik, ACS Med. Chem. Lett. 2021, 12, 502–507. DOI:10.1021/acsmedchemlett.1c00045
- J. Liu, D. W. Kang, Y. Fan, G. T. Nash, X. Jiang, R. R. Weichselbaum, W Lin, J. Am. Chem. Soc. 2024, 146, 849–857.
   DOI:10.1021/jacs.3c11092
- F. A. Kılıçarslan, A. Erdoğmuş, Ö. Budak, A. Koca, *Inorg. Chim. Acta* 2024, 561, 121870. DOI:10.1016/j.ica.2023.121870
- S. Aydogdu, A. Hatipoglu, A. Erdoğmuş, J. Comput. Biophys. Chem. 2022, 21, 599–609. DOI:10.1142/S2737416522500235

- M. Murali krishnan, S. Baskaran, M. N. Arumugham, *Inorg. Nano-Met. Chem.* 2021, *51*, 1165–1176.
   DOI:10.1080/24701556.2020.1815775
- M. Khazri, K. Sahra, A. Milet, B. Jamoussi, S. Messaoudi, J. Struct. Chem. 2020, 61, 844–851.
   DOI:10.1134/S0022476620060025
- J. M. Mir, N. Jain, P. S. Jaget, R. C. Maurya, *Photodiagnosis Photodyn. Ther.* 2017, 19, 363–374.
   DOI:10.1016/j.pdpdt.2017.07.006
- M. Lamač, D. Dunlop, K. Lang, P. Kubát, *J Photochem. Photobiol. A Chem.* 2022, 424, 113619.
   DOI:10.1016/j.jphotochem.2021.113619
- M. Khalid, M. U. Khan, S. Ahmed, Z. Shafiq, M. M. Alam, M. Imran, A. A. C. Braga, M. S. Akram, Sci. Rep. 2021, 11, 21540. DOI:10.1038/s41598-021-01070-3
- 20 A. Erdoğmus, T. Nyokong, *J. Mol. Struct.* **2010**, *977* (1–3), 26–38. **DOI:**10.1016/j.molstruc.2010.04.048
- A. Ram Kumar, S. Selvaraj, G. P. Sheeja Mol, M. Selvaraj, L. Ilavarasan, S. K. Pandey, P. Jayaprakash, S. Awasthi, O. Albormani, A. Ravi, *J. Mol. Liq.* 2024, 393, 123661.
   DOI:10.1016/j.molliq.2023.123661
- 22. E. S. Aazam, R. Thomas, *J. Mol. Liq.* **2024**, *395*, 123820. **DOI:**10.1016/j.molliq.2023.123820
- A. A. Otlyotov, I. V. Ryzhov, I. A. Kuzmin, Y. A. Zhabanov, M. S. Mikhailov, P. A. Stuzhin, *Int. J. Mol. Sci.* 2020, *21*, 2923. DOI:10.3390/ijms21082923
- M, Wierzchowski, L. Sobotta, D. Łażewski, Kasprzycki, P., Fita, P., Goslinski, T. *J. Mol. Struct.* 2020, *1203*, 127371.
   DOI:10.1016/j.molstruc.2019.127371
- I. D. Karagöz, Y, Yilmaz, K. Sanusi, J. Fluoresc. 2020, 30, 1151–1160. DOI:10.1007/s10895-020-02584-1/Published.
- M. J. Frisch, C. Adamo, A.J. Austin, et al. 2009, Gaussian 09 Revision B.01. Gaussian Inc., Wallingford
- 27. R. Dennington, T. Keith, J. Millam, **2009**, GaussView, Version 5, Semichem Inc., Shawnee Mission, KS.
- 28. J. Foresman, E. Frish Exploring chemistry. **1996**, Gaussian Inc, Pittsburg.
- 29. R. G. Parr, Y. Weitao, *Density Functional Theory of Atoms and Molecules*, **1995**, Oxford University Press: New York.
- R. K. Roy, N. Tajima, K. A Hirao, J. Phys. Chem. A, 2001, 105, 2117–2124. DOI:10.1021/jp0040087
- R. K. Roy, S. Pal, K. Hirao, J. Chem. Phys. 1999, 110, 8236–8245. DOI:10.1063/1.478792
- 32. C. C. Leznoff, A. B. P. Lever, *Phthalocyanines: Properties and applications*, **1989**, VCH, New York
- O. Bakaroglu, Appl. Organomet. Chem. 1996, 10, 605–622.
   DOI:10.1002/(SICI)1099-0739(199610)10:8<605::AID-AO-C527>3.0.CO;2-U
- 34. N. B. McKeown, Phthalocyanine materials: Synthesis, structure and function, **1998**, Cambridge University Press, Cambridge.
- 35. K. M. Kadish, K. M. Smith, R. Guilard, *The Porphyrin Hand-book Phthalocyanines: Spectroscopic and Electrochemical Characterization*, **2003**, Academic Press, Boston
- G. Socrates, Infrared and Raman Characteristic Group Frequencies: Tables and Charts, 2001, John Wiley and Sons: Chichester.

- 37. N. Sundaraganesan, S. Ilakiamani, H. Saleem, P. M. Wojciechowski, D. Michalska, *Spectrochim. Acta A Mol. Biomol. Spectrosc.* **2005**, *61*, 2995–3001. **DOI**:10.1016/j.saa.2004.11.016
- Ö. D. Kutlu, A. Erdoğmuş, P. Şen, S. Z. Yıldız, *J. Mol. Struct.* 2023, 1284, 135375. DOI:10.1016/j.molstruc.2023.135375
- A. M. Sevim, H. Y. Yenilmez, M. Aydemir, A. Koca, Z. A. Ba-yir, *Electrochim. Acta* 2014, *137*, 602–615.
   DOI:10.1016/j.electacta.2014.05.149
- P. Tau, T. Nyokong, *Electrochim. Acta* 2007, *52*, 3641–3650.
   DOI:10.1016/j.electacta.2006.10.023
- P. Koza, T. Koczorowski, D. T. Mlynarczyk, T. Goslinski, Zinc
   (II) Appl. Sci. 2022, 12, 6825.
   DOI:10.3390/app12136825
- 42. T. Nyokong, Coord. Chem. Rev. 2007, 251, 1707–1722. DOI:10.1063/1.334486
- 43. P. A Baruch, *J. Appl. Phys.* **1985**, *57*, 1347–1355. **DOI:**10.1063/1.334486.
- 44. A. C. Yüzer, G. Kurtay, T. Ince, S, Yurtdaş, E. Harputlu, K. Ocakoglu, M. Güllü, C. Tozlu, M. Ince, *Mater. Sci. Semicond. Process* **2021**, *129*, 105777. **DOI:**10.1016/j.mssp.2021.105777
- S. Samiee, P. Hossienpour, *Inorg. Chim. Acta* 2019, 494, 13–20. DOI:10.1016/j.ica.2019.05.006
- O. Britel, A. Fitri, A. T. Benjelloun, M. Benzakour, M. Mcharfi, *Struct. Chem.* 2023, 34, 1827–1842.
   DOI:10.1007/s11224-023-02122-2
- 47. J. Zhang, S. Peng, S. Zheng, *Mater. Chem. Phys.* **2021**, *263*, 124420. **DOI:**10.1016/j.matchemphys.2021.124420
- 48. S. Aydogdu, A. Hatipoglu, *Acta Chim. Slov.* **2022**, *69*, 647–656. **DOI:**10.17344/acsi.2022.7522
- I. Erden, A. Hatipoglu, C. Cebeci, S. Aydogdu, J. Mol. Struct.
   2020, 1201, 127202. DOI:10.1016/j.molstruc.2019.127202
- A. A. Piya, S. U. D. Shamim, M. N. Uddin, K. N. Munny, A. Alam, M. K. Hossain, F. Ahmed, *Comput. Theor. Chem.* 2021, 1200, 113241. DOI:10.1016/j.comptc.2021.113241
- 51. S. Aydogdu, A. Hatipoglu, *J. Indian Chem. Soc.* **2022**, 99, 100752. **DOI:**10.1016/j.jics.2022.100752

#### **Povzetek**

V prispevku opisujemo sintezo, karakterizacijo in elektronske lastnosti novih 4-((7-metoksikinolin-4-il)oksi), 4-(kinolin-2-iltio) in 4-((7-(trifluorometil)kinolin-4-il)tio) periferno substituiranih okso-titanovih ftalocianinov. Strukture spojin smo določili z metodami UV-Vis, FTIR, <sup>1</sup>H NMR in MALDI-TOF masno spektrometrijo. Elektronske spektre teh molekulske in elektronske lastnosti spojin smo izračunali z metodama teorije gostotnega funkcionala (DFT) in **časovno** odvisno teorijo gostotnega funkcionala (TD-DFT). Preučevali smo vpliv topila na elektronske in geometrijske lastnosti spojin in njihovo reaktivnost. Izračunali smo globalne in lokalne indekse reaktivnosti in molekularni elektrostatski potencial na površinah spojin. Reaktivnost in elektronska struktura molekul se spreminja v odvisnosti od topila in substituent. Ugotovili smo, da so sintetizirane spojine uporabne na različnih področjih, npr. za solarne celice ali v fotodinamični terapiji.



Except when otherwise noted, articles in this journal are published under the terms and conditions of the Creative Commons Attribution 4.0 International License